Z. Phys. C – Particles and Fields 51, 633–642 (1991)

Zeitschrift für Physik C Particles and Fields

Shadowing effects on quark and gluon production in ultrarelativistic heavy ion collisions

K.J. Eskola*
Department of Theoretical Physics, University of Helsinki, Siltavuorenpenger 20C, SF-00170 Helsinki, Finland

Received 4 February 1991

Abstract. A framework for including shadowing effects to quark and gluon production in very high energy nucleus-nucleus collisions is given. A formalism for impact parameter dependent nuclear structure functions of partons is introduced and, using two models to describe the average shadowing corrections to the parton number densities, the average numbers and the transverse energy spectrum of hard partons produced in $U+U$ collisions at RHIC and LHC energies are computed. We conclude that shadowing and also the impact parameter dependence of structure functions should be taken into account at very high energies.

1 Introduction

Hard QCD jets are clearly seen in pp and $p\bar{p}$ collisions from $\sqrt{s}\approx 50$ GeV upwards [1]. In heavy ion collisions at very high energies small p_T jets, "minijets", are still expected to be abundant but one cannot observe them due to the large multiplicities. Nevertheless, the produced quarks and gluons contribute to the evolution of the system the more the higher the energy is, as studied in [2–5]. The purpose of the present paper is to give a framework for estimating the effects of nuclear shadowing on the average number of produced quarks and gluons and on the transversal energy carried by them.

We define a minijet to be a quark or a gluon with $p_T \geqq p_0$, where p_0 is the scale above which perturbative QCD is valid. We expect that $p_0 \sim 2$ GeV [2]. The dynamical meaning of p_0 and its possible A- and $\sqrt{s}$-dependence are discussed in [6]. We are going to give the numbers of quarks and gluons as functions of p_0 in order to see the sensitivity of the results to this scale. How much varying the scale p_0 affects the transverse energy spectrum is shown in [7].

At high energies the produced minijets are mainly gluons with $p_T \sim p_0$. In a pp subcollision at $\sqrt{s}=200$ GeV the typical x's of partons are $2p_T/\sqrt{s}\sim 0.02$, and $\sim 5\cdot 10^{-4}$ for $\sqrt{s}=7000$ GeV. The small-x region of the nuclear structure functions becomes thus more important with increasing energy. EMC data reveals a clear depletion of f_A at small x relative to Af for the structure function F_2 [8, 9]. Therefore, approximating the nuclear structure functions only by $f_A = Af$ is not sufficient; corrections to this should be included. There are several models how the depletion in the data is caused by parton shadowing (see e.g. Refs. of [10]). For quarks and antiquarks the various models can be tested, using data for $F_2(A)/F_2(D)$, but the gluon situation is, unfortunately, worse: no direct data on g_A/Ag is available.

The first goal of this paper is to study to what extent nuclear shadowing decreases the number of quarks and gluons in $A+A$, when compared to the calculations without any shadowing in [2]. The second one is to study whether nuclear shadowing has a significantly larger effect on the central collisions (zero impact parameter) compared to the averaged ones. Inside an incoming nucleus there are more partons in the center of the nucleus than near the peripheral regions. Hence one would expect stronger shadowing to take place in this central region, and, therefore also stronger reduction of the parton densities. This leads to the idea that in central collisions, i.e. in collisions where the centers of the nuclei collide onto each other, minijet production would be relatively more suppressed than in average collisions. This is what we call "central shadowing". The third goal is to compute the consequences of the reduction in the parton densities to the transversal energy distribution of minijets and to find out when central shadowing is an important effect.

In Sect. 2 a formalism is developed for nuclear structure functions $\Gamma_A(x, p_T^2, \mathbf{s})$ which depend on the transversal location $\mathbf{s}$ of the partons inside a nucleus, and thereby also on the impact parameter. This microscopic model is based on parton overlapping. A formalism for the average numbers of jets from $A+A$ collisions is given, as well as a definition for central shadowing. In Sect. 3 the impact parameter dependent structure function formalism is applied to the transversal energy distribution $d\sigma/dE_T$ of minijets. In Sects. 4 and 5 we compute the

* kjeskola@finuhcb.bitnet

average numbers of produced partons from $U+U$ and the final transversal energy spectrum by using the formalism in Sects. 2 and 3. Also the central shadowing effects are studied. The computations are carried out for two interesting energies: LHC, $\sqrt{s}=7000\,A\,\mathrm{GeV}$ and RHIC, $\sqrt{s}=200\,A\,\mathrm{GeV}$.

In Sects. 2 and 3 we assume that the depletion in f_A/Af is known separately for the different parton species. While this not the case for gluons, and not even for quarks in as large nuclei as U, we use as a starting point in Sect. 4 a qualitative approach for obtaining this ratio. There we introduce a simplified Ansatz for f_A/Af at small x (motivated by the EMC data) that we can vary in an appropriate way. This is closely related to that of Qiu in [15], though somewhat simplified, containing no scale dependence. In Sect. 5 we then improve the picture by extrapolating to $A=U=238$ for quarks and antiquarks from the existing F_2 data [9, 12] in the whole x range. To describe the unknown gluon structure function g_U we apply the initial state recombination model of Close et al. [11]. In this model the modifications to g_U vanish quickly ($\sim 1/Q^2$) with increasing scale.

Finally, the results are discussed in Sect. 6. The most crucial fact from the point of view of the shadowing effects turns out to be the behaviour of shadowing corrections to the gluon structure function. If these do not get strongly suppressed with increasing scale, shadowing causes a large effect, factor 2, to the jet numbers and E_T distributions at high energies like in the LHC. In this case central shadowing effects, caused by the impact parameter dependence of the structure functions, should also be taken into account.

2 Impact parameter dependent structure functions

In this section we first introduce a formalism for impact parameter dependent nuclear structure functions. Using these we calculate the number of minijets produced both in central and in average $A+A$ collisions and finally we study central shadowing effects.

Let us take the calculations in [2] as a starting point. In the first approximation it is assumed that nuclear geometry and QCD are factorizable and that the 2-jet QCD-processes are dominant. Then, the average number of hard minijets (partons) in an $A+A$ collision at fixed impact parameter $\mathbf{b}$ is obtained as a product of the standard nuclear overlap functions $T_{AA}(\mathbf{b})$ and the inclusive 2-jet cross section integrated over the momenta, $\langle n_{\mathrm{jet}}(n_{\mathrm{jet}}-1)\rangle\,\sigma_{pp}^{\mathrm{QCD}}(p_0)\approx 2\sigma_{pp}^{\mathrm{QCD}}(p_0)$,

$$n_{AA}^0(\mathbf{b})=2\,T_{AA}(\mathbf{b})\sigma_{pp}^{\mathrm{QCD}}(p_0)$$
$$=\int_{p_0^2}\mathrm{d}p_T^2\,\mathrm{d}y_1\,\mathrm{d}y_2\,\mathrm{d}^2\mathbf{s}_1\,\mathrm{d}^2\mathbf{s}_2\,\delta^2(\mathbf{b}-\mathbf{s}_1-\mathbf{s}_2)\frac{\mathrm{d}\sigma^{gg}}{\mathrm{d}\hat{t}}$$
$$\cdot x_1\Gamma_A^0(x_1,p_T^2,\mathbf{s}_1)\,x_2\Gamma_A^0(x_2,p_T^2,\mathbf{s}_2). \tag{1}$$

In this approximation the impact parameter dependent nuclear structure function is defined as

$$\Gamma_A^0(x,p_T^2,\mathbf{s})=T_A(\mathbf{s})f(x,p_T^2), \tag{2}$$

where the thickness function $T_A(\mathbf{s})$ is a longitudinal integral over the nuclear density n_A and it is normalized to A:

$$T_A(\mathbf{s})=\int_{-\infty}^{\infty}\mathrm{d}z\,n_A(\sqrt{\mathbf{s}^2+z^2}),\quad \int\mathrm{d}^2\mathbf{s}\,T_A(\mathbf{s})=A. \tag{3}$$

The index 0 in n_{AA}^0 and Γ_A^0 is to indicate that nuclear effects are not included. This means that the nuclear parton structure function is A times the nucleon structure function. From (2)

$$f_A^0(x,p_T^2)\equiv\int d^2\mathbf{s}\,\Gamma_A^0(x,p_T^2,\mathbf{s})=Af(x,p_T^2). \tag{4}$$

Following [2], the QCD minijet cross section is computed by approximating the various parton-parton subprocesses by [14]

$$f(x,p_T^2)=g(x,p_T^2)+\tfrac{4}{9}\sum_f[q_f(x,p_T^2)+\bar{q}_f(x,p_T^2)] \tag{5}$$

and by using the Duke-Owens soft gluon structure functions with $\Lambda_{\mathrm{QCD}}=200$ MeV and the scale $Q=p_T$ [13].

To get the number of partons produced in an *average* $A+A$ collision we integrate (1) over all impact parameters and divide by the total inelastic AA cross section:

$$\bar{n}_{AA}^0=\frac{A^2}{4\pi R_A^2}\int_{p_0^2}\mathrm{d}p_T^2\,\mathrm{d}y_1\,\mathrm{d}y_2\frac{\mathrm{d}\sigma^{gg}}{\mathrm{d}\hat{t}}\,x_1f(x_1,p_T^2)\,x_2f(x_2,p_T^2). \tag{6}$$

In the following we shall discuss the nuclear shadowing corrections to the parton number densities. In a qualitative picture [15] shadowing begins at $x_N\equiv 1/(2m_Nr_N)\approx 0.1$ when partons in neighbouring nucleons start to overlap. A region of complete shadowing in this picture would then exist at $x\lesssim x_A\equiv 1/(2m_NR_A)\sim 0.01$ fm for $A\sim 200$, i.e. when the partons are spread longitudinally over the whole contracted nucleus. We have denoted by m_N the mass of the nucleon, by r_N the radius of the nucleon and by R_A the radius of the nucleus.

Let us now consider a correction term $\Delta\Gamma_A$ to the impact parameter dependent structure function in (2). We expect that the correction $\Delta\Gamma_A$ is mainly due to two-particle interactions of longitudinally overlapping partons at $\mathbf{s}$. The number of nucleons and thus the number of partons at $\mathrm{d}^2\mathbf{s}$ in a nucleus A is proportional to $T_A(\mathbf{s})$. Therefore we write the correction term as follows:

$$\Gamma_A(x,p_T^2,\mathbf{s})=\Gamma_A^0(x,p_T^2,\mathbf{s})+\Delta\Gamma_A(x,p_T^2,\mathbf{s})$$
$$=f(x,p_T^2)\,T_A(\mathbf{s})+\Phi_2^A(x,p_T^2)[T_A(\mathbf{s})]^2, \tag{7}$$

where Φ_2^A is the correction term coefficient depending on x and on the scale $Q=p_T$. The dimension of Φ_2^A is fm^2 and the index A refers to the possible A dependence that the coefficient has through x_A. When writing such a form for $\Delta\Gamma_A$ we actually assume that *any* parton at $\mathbf{s}$ in a nucleus A can overlap and thereby also interact with any other parton at the same $\mathbf{s}$. However, this is true only if the x's of the partons are small enough but not necessarily if the x's are large. It would be quite

possible to introduce a weight function which suppresses the correction at large x's for partons spatially far apart, as was done in [11]. Nevertheless, at this point we want to keep things as simple as possible and appeal again to the fact that most of the minijets are due to small x gluons, being able to overlap with the other partons.

Integration over the transverse area gives the 'usual' nuclear structure function. Let us also define the "shadowing function" S_A^f as follows:

$$f_A(x,p_T^2)\equiv\int d^2\mathbf{s}\,\Gamma_A(x,p_T^2,\mathbf{s})\equiv A f(x,p_T^2)\,S_A^f(x,p_T^2)$$
$$=A f(x,p_T^2)+\Phi_2^A(x,p_T^2)\int d^2\mathbf{s}[T_A(\mathbf{s})]^2. \tag{8}$$

Solving for Φ_2^A and inserting to (7) we obtain

$$\Gamma_A(x,p_T^2,\mathbf{s})=f(x,p_T^2)\,T_A(\mathbf{s})\left\{1-\frac{AT_A(\mathbf{s})}{N_A}\left[1-S_A^f(x)\right]\right\}, \tag{9}$$

where $N_A\equiv\int d^2\mathbf{s}[T_A(\mathbf{s})]^2$.

If the A dependence of $1-S_A^f$ could precisely be measured, one would be able to test the assumption about the dominating two-particle interactions. In here this quantity scales like $A^{1/3}$, as it is usually assumed [11, 15, 19, 20]. However, when x gets small enough, also many particle interactions may become important [18].

The average number of minijets in such a collision at fixed impact parameter $\mathbf{b}$ is now with (8)

$$n_{AA}(\mathbf{b})=\int_{p_0^2} dp_T^2\,dy_1\,dy_2\,d^2\mathbf{s}\,\frac{d\sigma^{gg}}{d\hat{t}}\,x_1\Gamma_A(x_1,p_T^2,\mathbf{s})$$
$$\cdot x_2\Gamma_A(x_2,p_T^2,\mathbf{b}-\mathbf{s}), \tag{10}$$

where $\Gamma_A=\Gamma_A^g+\frac{4}{9}\sum_f[\Gamma_A^f+\Gamma_A^{\bar{f}}]$.

Averaging over the impact parameter in the same manner as in (6) leads directly from (10) to the number of minijets in an average $A+A$ collision:

$$\bar{n}_{AA}=\frac{1}{4\pi R_A^2}\int_{p_0^2} dp_T^2\,dy_1\,dy_2\,d^2\mathbf{s}\,\frac{d\sigma^{gg}}{d\hat{t}}\,x_1 f_A(x_1,p_T^2)$$
$$\cdot x_2 f_A(x_2,p_T^2), \tag{11}$$

where $f_A=AS_A^g g+\frac{4}{9}A\sum_f[S_A^q q_f+S_A^{\bar{q}}q_{\bar{f}}]$, respectively.

Finally we discuss the concept of central shadowing. We have assumed above that the reduction in the nuclear parton densities is the larger the more there are partons longitudinally overlapping at $\mathbf{s}$ inside a nucleus A. It is then in the central region of the nucleus near $\mathbf{s}\sim\mathbf{0}$ that the parton densities are most suppressed. This is why we expect that minijet production in central collisions ($\mathbf{b}\sim\mathbf{0}$) is more suppressed than in averaged (over $\mathbf{b}$) collisions. Let us define a quantity $C(p_0)$, which characterizes the extent of central shadowing:

$$C(p_0)\equiv 1-\frac{n_{AA}(\mathbf{0})/n_{AA}^0(\mathbf{0})}{\bar{n}_{AA}/\bar{n}_{AA}^0}. \tag{12}$$

This definition is not sensitive for any multiplicative factors in the jet numbers. This is useful since, e.g., K-factors cannot be uniquely defined.

3 E_T distribution

Next we shall apply the impact parameter dependent structure function formalism of the previous section to the transversal energy distribution $d\sigma/dE_T$ of minijets in $A+A$ collisions. The simplest way of including nuclear shadowing effects would be just to replace Af by $AS_A^f f$ as was done in (11). This gives a first estimate of the order of the shadowing corrections to $d\sigma/dE_T$ and is given in [7] (see also Fig. 4). However, we expect that minijet production at high energies is more suppressed in central $A+A$ collisions than in peripheral ones. This reflects also to the E_T spectrum of quarks and gluons.

Following [2, 3] again, we assume that the hard nucleon-nucleon subcollisions in $A+A$ are independent. The average number of hard sub*collisions* at fixed impact parameter is obtained from (10) as $N_{AA}(\mathbf{b})=\frac{1}{2}n_{AA}(\mathbf{b})$, since the 2-jet QCD-processes were assumed to dominate. Thus $N_{AA}(\mathbf{b})$ collisions are expected to occur, while the actual number of hard collisions in $A+A$ is N with a Poissonian probability. Now the transverse energy distribution of each of the N subcollisions depends on the transversal location, i.e. on the impact parameter. The total E_T distribution of the produced (mini)jets becomes then

$$\frac{d\sigma_h^{AA}}{dE_T}=\int d^2\mathbf{b}\sum_1^\infty\frac{[N_{AA}(\mathbf{b})]^N}{N!}\exp[-N_{AA}(\mathbf{b})]$$
$$\cdot\int\prod_1^N dE_{Ti}\,\frac{1}{N_{AA}(\mathbf{b})}\frac{dN_{AA}(\mathbf{b})}{dE_{Ti}}\,\delta\left(E_T-\sum_1^N E_{Ti}\right), \tag{13}$$

where the normalized E_T spectrum of one subcollision is given by $1/N_{AA}(\mathbf{b})\,dN_{AA}(\mathbf{b})/dE_T$. Note that the number of *subcollisions* does not depend on any acceptance of the apparatus, but the number of *observed* minijets does. If one wants to include kinematical cuts e.g. in rapidity and/or in azimuthal angle, it is only in $dN_{AA}(\mathbf{b})/dE_T$ that this shows:

$$\frac{dN_{AA}(\mathbf{b})}{dE_T}=\int_{p_0^2} dp_T^2\,dy_1\,dy_2\,\frac{d\phi}{2\pi}\,d^2\mathbf{s}\,\delta(E_T-(\varepsilon_1+\varepsilon_2)\,p_T)$$
$$\cdot\frac{1}{2}\frac{d\sigma^{gg}}{d\hat{t}}\,x_1\Gamma_A(x_1,p_T^2,\mathbf{s})\,x_2\Gamma_A(x_2,p_T^2,\mathbf{b}-\mathbf{s}). \tag{14}$$

For brevity we have used above the notation of [2] for the indicators:

$$\varepsilon_1\equiv\varepsilon(y_1,\phi)=\begin{cases}1, & \text{jet 1 in the detector;}\\ 0, & \text{jet 1 outside,}\end{cases} \tag{15}$$

and $\varepsilon_2\equiv\varepsilon(y_2,\phi+\pi)$ for jet 2, respectively. Note also that (14) is normalized to $N_{AA}(\mathbf{b})$: the unobserved partons contribute to the $\delta(E_T)$ term.

For $E_T>0$ the expression (13) is approximately a gaussian distribution

$$\frac{d\sigma_h^{AA}}{dE_T}=\int d^2\mathbf{b}\,\frac{1}{\sqrt{2\pi\sigma_h^2(\mathbf{b})}}\exp\left\{-\frac{[E_T-\bar{E}_{T,h}^{AA}(\mathbf{b})]^2}{2\sigma_h^2(\mathbf{b})}\right\}, \tag{16}$$

where

$$\bar{E}_{T,h}^{AA}(\mathbf{b}) = N_{AA}(\mathbf{b}) \langle E_T \rangle_h^{pp} = \int \mathrm{d}E_T E_T \frac{\mathrm{d}N_{AA}(\mathbf{b})}{\mathrm{d}E_T} \tag{17}$$

$$\sigma_h^2(\mathbf{b}) = N_{AA}(\mathbf{b}) \langle E_T^2 \rangle_h^{pp} = \int \mathrm{d}E_T E_T^2 \frac{\mathrm{d}N_{AA}(\mathbf{b})}{\mathrm{d}E_T}. \tag{18}$$

The soft component can then be added to these hard quantities as in [2], in order to estimate the final E_T-distribution of an $A+A$ collision. This is done in Sects. 4 and 5.

4 Model I: effective shadowing function

In the following sections we shall apply two models for the shadowing functions S_A^f. By using these models we compute the average numbers of produced minijets in a $U+U$ collision and study the final E_T distribution.

Most of the produced minijets are gluons and their share increases when going to higher energies [16]. Therefore we need especially the nuclear structure functions for gluons but, unfortunately, there does not exist any data for g_A or g_A/Ag. Motivated by the EMC data for the structure function F_2 [8, 9], let us introduce the following simple ansatz for an effective shadowing function S_A, which is closely related to that of Qiu in [15]:

$$S_A(x) \equiv \frac{f_A(x, p_T^2)}{A f(x, p_T^2)} = \begin{cases} 1, & x \geqq x_N; \\ 1 - \mathscr{K}_A s(x), & x_A < x < x_N; \\ 1 - \mathscr{K}_A s(x_A), & x \leqq x_A, \end{cases} \tag{19}$$

where $\mathscr{K}_A$ is a parameter that describes the A-dependence of shadowing at $x_A < x < x_N$. Shadowing in the complete shadowing region is characterized here by a parameter $K_A \equiv \mathscr{K}_A s(x_A)$, determined by the interaction mechanism of partons and the size of the nucleus. Since both $\mathscr{K}$ and K_A are essentially unknown, we shall vary K_A from 0.5 down to 0. The function $s(x)$ we define so that $s(x_N)=0$, i.e. we simply assume that shadowing begins at x_N (for a possible A dependence of x_N, see [17]). Because the data [9] for the ratio $F_2(A)/F_2(D)$ does not show any clear scale dependence, we assume also S_A to be scale independent. (The scale dependence of this kind of an ansatz was studied by Qiu in [15]). We shall be content with a function $s(x) = \ln(x_N/x)$, reproducing reasonably well the shape of the F_2-data ion [8, 9] at small x. Furthermore, we shall assume that the depletion is of the same size and of the same form for gluons and quarks. Note also that to maintain the parton momentum sum rule a more detailed model should be applied, such as in [10, 11, 18]. Since practically only the small x region is important for minijet production, the sum rule violation can be neglected here.

By using the expression (9) the average number of minijets in an $A+A$ collision at fixed $\mathbf{b}$ ((10)) can be put into the following form:

$$n_{AA}(\mathbf{b}) = n_{AA}^0(\mathbf{b}) \left\{ 1 - b_2(\mathbf{b}) \left[1 - \frac{\sigma_s(p_0)}{\sigma(p_0)} \right] - c_2(\mathbf{b}) \left[1 - \frac{\sigma_{ss}(p_0)}{\sigma(p_0)} \right] \right\}, \tag{20}$$

where $n_{AA}^0(\mathbf{b}) = 2 T_{AA}(\mathbf{b}) \sigma(p_0)$ from (1) and $\sigma(p_0) \equiv \sigma_{pp}^{\mathrm{QCD}}(p_0)$. The cross section integrals containing the shadowing function are denoted above by

$$\sigma_s(p_0) \equiv \int_{p_0^2} \mathrm{d}p_T^2 \mathrm{d}y_1 \mathrm{d}y_2 \frac{1}{2} \frac{\mathrm{d}\sigma_h^0}{\mathrm{d}p_T^2 \mathrm{d}y_1 \mathrm{d}y_2} S_A(x_1), \tag{21}$$

and

$$\sigma_{ss}(p_0) \equiv \int_{p_0^2} \mathrm{d}p_T^2 \mathrm{d}y_1 \mathrm{d}y_2 \frac{1}{2} \frac{\mathrm{d}\sigma_h^0}{\mathrm{d}p_T^2 \mathrm{d}y_1 \mathrm{d}y_2} S_A(x_1) S_A(x_2), \tag{22}$$

where $\mathrm{d}\sigma_h^0/\mathrm{d}p_T^2 \mathrm{d}y_1 \mathrm{d}y_2 = x_1 f(x_1, p_T^2)\, x_2 f(x_2, p_T^2)\, \mathrm{d}\sigma^{gg}/\mathrm{d}\hat{t}$. The impact parameter dependent coefficients are the following:

$$b_2(\mathbf{b}) = \frac{2A}{N_A T_{AA}(\mathbf{b})} \left[T_{AA^2}(\mathbf{b}) - \frac{A T_{A^2A^2}(\mathbf{b})}{N_A} \right],$$

$$c_2(\mathbf{b}) = \frac{A^2 T_{A^2A^2}(\mathbf{b})}{N_A^2 T_{AA}(\mathbf{b})}, \tag{23}$$

where $T_{AA^2}(\mathbf{b}) \equiv \int \mathrm{d}^2\mathbf{s} [T_A(\mathbf{s})]^2 T_A(\mathbf{b}-\mathbf{s})$ and $T_{A^2A^2}(\mathbf{b}) \equiv \int \mathrm{d}^2\mathbf{s} [T_A(\mathbf{s})]^2 [T_A(\mathbf{b}-\mathbf{s})]^2$. In the numerical calculation of these coefficients we use the Woods-Saxon parametrization [21] (see also appendix of [2]).

In Fig. 1 we show the average number of jets with $p_T \geqq p_0$ in a central $U+U$ collision according to (12) as a function of p_0. All rapidities are accepted here. The results with $K_U = 0.3$ and 0.5 correspond to the solid curves, and the first approximation without any shadowing ($K_U = 0$) from (1) to the dashed ones. The curves are plotted for two interesting energies: RHIC $\sqrt{s} = 200\ A$GeV and LHC $\sqrt{s} = 7000\ A$GeV. In this calculation we have not taken into account the higher order QCD corrections [22], i.e. we have set the K-factor to unity. (For $\mathrm{d}\sigma/\mathrm{d}p_T\,\mathrm{d}y(y=0)$ at $\sqrt{s} = 200$ GeV in pp-collisions we expect a K-factor of ~ 2.5 and less for $\sqrt{s}$

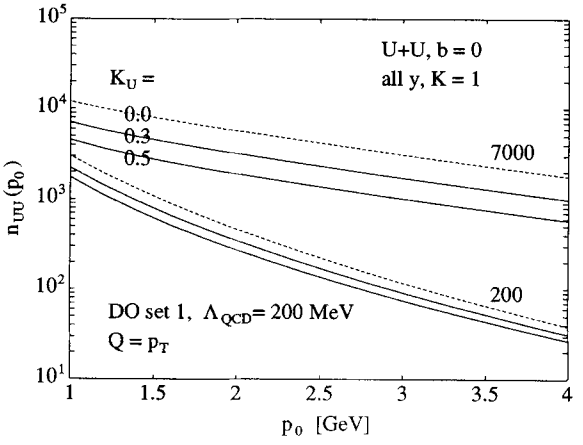

Fig. 1. The average number of jets with $p_T \geqq p_0$, any rapidity, from a central $U+U$ collision at $\sqrt{s} = 7000\ A$GeV and $200\ A$GeV, as computed from (20) with $\mathbf{b}=\mathbf{0}$. The solid lines show the numbers for $K_U = 0.3$ and 0.5, and the dashed ones for $K_U = 0$ case (i.e. no shadowing). Duke-Owens soft gluon structure function set with $\Lambda_{\mathrm{QCD}} = 200$ MeV and with the scale $Q^2 = p_T^2$ was used [13]. The order α_s^3-terms [22] were not included ($K=1$)

$=1800$ [1, 2, 23]). At 7000 AGeV about 1900 (3200) jets with $p_T \geqq 2$ GeV and any rapidity are produced, corresponding to $K_U=0.5$ (0.3). At 200 AGeV we get 270 (342) jets, respectively. The nonshadowed numbers at $p_0=2$ GeV are reduced by 67 (44)% for $K_U=0.5$ (0.3) at the LHC energy and by 41 (26)% at the RHIC energy. The relative amount of shadowing at high energies does not vary much with p_0's shown. This is due to the fact that the most important x-region, $2p_0/\sqrt{s}$, is of the same order with all these p_0's. Since the shadowing function here does not depend on the scale p_T, we get the same relative contribution with each p_0.

The impact parameter dependence of the average number of jets with $p_T \geqq 2$ GeV, any rapidity, from $U+U$ is illustrated in Fig. 2. There $n_{AA}(\mathbf{b}, p_0=2\text{ GeV})$ is displayed as a function of $\mathbf{b}$ at $\sqrt{s}=200$ and 7000 AGeV for different K_U's (solid lines). Also these curves are compared to $K_U=0$ predictions (dashed lines). The jet number is relatively more suppressed in the vicinity of $\mathbf{b}\sim\mathbf{0}$ than at large $\mathbf{b}$.

The average number of minijets in an average $A+A$ collision is according to (11) and (19) given by $\bar{n}_{AA}(p_0) = A^2\sigma_{ss}(p_0)/4\pi R_A^2$. This is plotted for $U+U$ in Fig. 3 versus p_0 with the K_U values 0.3 and 0.5 at the LHC and RHIC energies (solid lines). The result of (6) corresponds to the dashed lines. The average jet numbers for $p_0=2$ GeV are 564 (879) at $\sqrt{s}=7000$ AGeV and 75 (92) at $\sqrt{s}=200$ AGeV with $K_U=0.5$ (0.3). The respective suppression from the nonshadowed case are 61 (40)% for $K_U=0.5$ (0.3) and 37 (23)%. Since no cuts in the jet repidities were imposed, the effect is less than $1-(1-K_U)^2$.

The definition (12) for central shadowing can be written in the following form by using (1), (6) and (20–23):

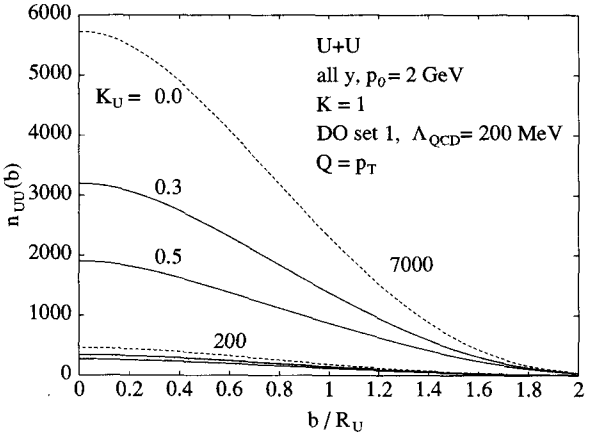

Fig. 2. The impact parameter dependence of the average number of jets with $p_T \geqq 2$ GeV, any rapidity from a $U+U$ collision at $\sqrt{s}=7000$ AGeV and 200 AGeV, as predicted by (20). The impact parameter $\mathbf{b}$ is in units of $R_U \approx 6.8$ fm. The solid lines corresponds to $K_U=0.3$ and 0.5, and the dashed ones to $K_U=0$. For LHC energy central shadowing is seen; minijet production in the region near $\mathbf{b}\sim\mathbf{0}$ is relatively more suppressed than in the peripheral region at large $\mathbf{b}$. The numbers at $\mathbf{b}=\mathbf{0}$ correspond to the numbers at $p_0=2$ GeV in Fig. 1

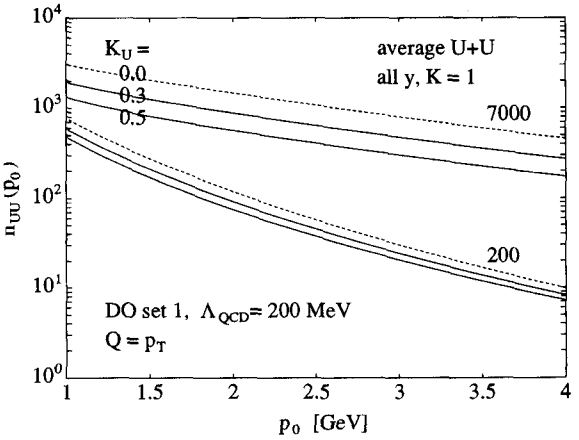

Fig. 3. The average number of minijets ($p_T \geqq p_0$, all y's) from an average $U+U$ collision. The averaging over the impact parameter is carried out acording to (11). The notations, energies and parameter values are the same as in Figs. 1 and 2

$$C(p_0)=\left\{\frac{\sigma_{ss}(p_0)}{\sigma(p_0)}\right\}^{-1}\cdot\left\{b_n(\mathbf{0})\left[1-\frac{\sigma_s(p_0)}{\sigma(p_0)}\right]+[c_n(\mathbf{0})-1]\left[1-\frac{\sigma_{ss}(p_0)}{\sigma(p_0)}\right]\right\}. \tag{24}$$

From the jet numbers in Figs. 1 and 3 we obtain that $C(p_0=2\text{ GeV})\approx 0.14$ (0.07) for $\sqrt{s}=7000$ AGeV with $K_U=0.5$ (0.3), i.e. in central collisions minijet production is suppressed 14 (7)% more as in average ones. For $\sqrt{s}=200$ AGeV $C(p_0=2\text{ GeV})$ is reduced to 0.07 (0.04), respectively. Thus, if shadowing corrections to the gluon structure functions are large ($\sim 50\%$) at small x, the impact parameter dependence of the structure functions should be taken into account.

Finally, we compute the transverse energy spectrum $\mathrm{d}\sigma^{AA}/\mathrm{d}E_T$ of a $U+U$ collision according to Sect. 3. We add the soft contribution to (17) and (18) by using the estimates for the first and second soft E_T-moments in a pp-collision from [2]. Thus the final E_T spectrum is given by (16) with

$$\bar{E}_T^{AB}(\mathbf{b})=T_{AA}(\mathbf{b})\left\{\sigma(p_0)\langle E_T\rangle_0^{pp}\left[1-b_2(\mathbf{b})\cdot\left(1-\frac{\langle E_T\rangle_s^{pp}\sigma_s(p_0)}{\langle E_T\rangle_0^{pp}\sigma(p_0)}\right)-c_2(\mathbf{b})\cdot\left(1-\frac{\langle E_T\rangle_{ss}^{pp}\sigma_{ss}(p_0)}{\langle E_T\rangle_0^{pp}\sigma(p_0)}\right)\right]+15\text{ mbGeV}\right\}, \tag{25}$$

$$\sigma^2(\mathbf{b})=T_{AA}(\mathbf{b})\left\{\sigma(p_0)\langle E_T^2\rangle_0^{pp}\left[1-b_2(\mathbf{b})\cdot\left(1-\frac{\langle E_T^2\rangle_s^{pp}\sigma_s(p_0)}{\langle E_T^2\rangle_0^{pp}\sigma(p_0)}\right)-c_2(\mathbf{b})\cdot\left(1-\frac{\langle E_T^2\rangle_{ss}^{pp}\sigma_{ss}(p_0)}{\langle E_T^2\rangle_0^{pp}\sigma(p_0)}\right)\right]+50\text{ mbGeV}^2\right\}, \tag{26}$$

where we have used the notations of (20) and ($m=1,2$)

$$\langle E_T^m\rangle_0^{pp}\,\sigma(p_0) = \int_{p_0^2} \mathrm{d}p_T^2\,\mathrm{d}y_1\,\mathrm{d}y_2\,\frac{\mathrm{d}\phi}{2\pi}(\varepsilon_1+\varepsilon_2)^m p_T^m\,\frac{1}{2}\,\frac{\mathrm{d}\sigma_h^0}{\mathrm{d}p_T^2\,\mathrm{d}y_1\,\mathrm{d}y_2}, \tag{27}$$

$$\langle E_T^m\rangle_s^{pp}\,\sigma_s(p_0) = \int_{p_0^2} \mathrm{d}p_T^2\,\mathrm{d}y_1\,\mathrm{d}y_2\,\frac{\mathrm{d}\phi}{2\pi}(\varepsilon_1+\varepsilon_2)^m p_T^m\,\frac{1}{2}\,\frac{\mathrm{d}\sigma_h^0}{\mathrm{d}p_T^2\,\mathrm{d}y_1\,\mathrm{d}y_2}\,S_A(x_1), \tag{28}$$

$$\langle E_T^m\rangle_{ss}^{pp}\,\sigma_{ss}(p_0) = \int_{p_0^2} \mathrm{d}p_T^2\,\mathrm{d}y_1\,\mathrm{d}y_2\,\frac{\mathrm{d}\phi}{2\pi}(\varepsilon_1+\varepsilon_2)^m \cdot p_T^m\,\frac{1}{2}\,\frac{\mathrm{d}\sigma_h^0}{\mathrm{d}p_T^2\,\mathrm{d}y_1\,\mathrm{d}y_2}\,S_A(x_1)\,S_A(x_2). \tag{29}$$

Note that we may have slightly overestimated the A scaling of the soft contribution in (25) and (26), when approximating that also the soft contribution scales with $T_{AA}\sim A^{4/3}$. This does not, however, matter as at high energies the respective scaling of the rapidity distribution $\mathrm{d}N_{AA}/\mathrm{d}y = A^{1+\alpha}\mathrm{d}N_{pp}/\mathrm{d}y$ is found to be $A^{1+\alpha}$ with $\alpha\sim 0.2$ for large nuclei [29].

In Fig. 4 we have displayed the final E_T-distribution for a $U+U$ collision at $\sqrt{s}=200$ and 7000 AGeV. Jets with $|y|\leqq 0.5$ (all ϕ) and $p_T\geqq 2$ GeV were accepted. Distributions with central shadowing are shown by solid curves and the nonshadowed ones with dashed lines. At RHIC energies shadowing reduces the average E_T by 15 (10)% for $K_U=0.5$ (0.3), while at the LHC energies the effect may be remarkable, even more than 50 (30)% for $K_U=0.5$ (0.3). Thus shadowing effects are clearly smaller at RHIC energies than at LHC energies. This is because at smaller energies one does not reach that low x's as at higher energies, and, because the relative share of soft component in the total $\langle E_T\rangle$ is larger at smaller energies.

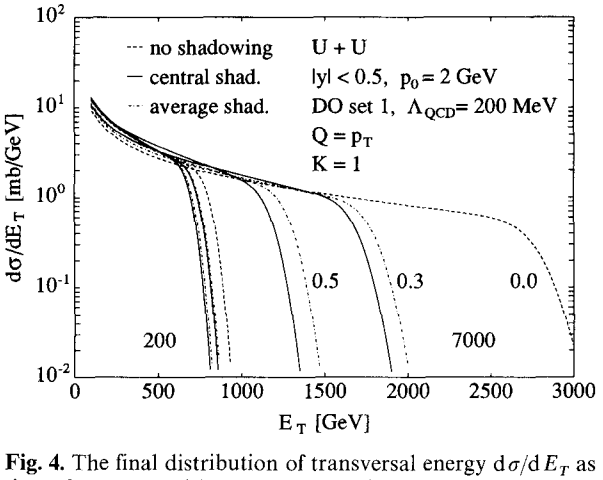

Fig. 4. The final distribution of transversal energy $\mathrm{d}\sigma/\mathrm{d}E_T$ as function of E_T. Jets with $p_T\geqq 2$ GeV and $|y|\leqq 0.5$ were accepted. The distributions are shown for $\sqrt{s}=7000$ AGeV and 200 AGeV. The solid curves stand for impact parameter dependent shadowing with $K_U=0.3$ and 0.5. These distributions contain the shadowing corrected hard part as well as the soft contribution, (25–29). The dotted-dashed curves correspond to the case where only average structure functions AfS_A (cf. (8)) are used [7, 23], i.e. shadowing in here does not depend on the impact parameter. The dashed lines describe the results without any nuclear modifications to the parton structure functions

The dotted-dashed lines in Fig. 4 describe the case in which we have, instead of using the impact parameter dependent structure functions (9), replaced Af by the average AS_Af [7]. As expected, at RHIC energies central shadowing is not an important effect, and the average treatment with AS_Af's describes the situation well. At LHC energies – where shadowing is an important suppression effect – central shadowing begins to show: to the average case it causes an additional reduction of 10 (6)% in the average E_T.

5 Model II: extrapolation from data and CQR gluons

In the previous section we have studied the shadowing effects on minijet production with a simple ansatz (19) for the shadowing function. In this section, we shall apply more detailed shadowing functions, different for quarks and gluons and containing modifications to the ratio f_A/Af in the whole x range. The quark-antiquark part, S_U^q, will be extrapolated from existing nuclear data for the structure functions F_2 [8, 9, 12]. The more uncertain gluonic part, S_U^g, is obtained by applying the initial state recombination model of Close et al. [11], where the modifications to the gluon structure function are dominantly due to two-gluon fusion and depend strongly on the scale. Also in this section we shall form the impact parameter dependent structure functions according to Sect. 2.

The corrections to the quark and antiquark structure functions are estimated in the following way. The small x data of $F_2(A)/F_2(D)$ exists for Ca [9]. We fit a straight line in a $\log(x)$-scale to the data below $x=0.1$ (ignoring one point, see Fig. 5) by keeping the point at $x=0.1$ fixed to 0. Assuming again that the slope of the correction term scales as $A^{1/3}$ we can extrapolate the curve for U. If the complete shadowing region exists, as we here shall assume, the data shows that $x_{\mathrm{Ca}}\lesssim 4\cdot 10^{-3}$ for Ca. The corresponding value for U we get by scaling by $A^{-1/3}$, which gives $x_U=(40/238)^{1/3}\cdot 0.004\approx 2.2\cdot 10^{-3}$. Then we use the Au data from [12] and on a linear scale fit a straight line to the EMC region $x\sim 0.15-0.7$ and a parabola to the five last points. Since the EMC region scales only as $\log(A)$ and the large x region does not practically contribute to minijet production at high energies, we use the resulting curve for Au directly for U. The total, impact parameter averaged ratio of structure functions F_2 becomes then for U as:

$$\frac{F_2(U)}{F_2(D)} \equiv S_U^q(x) \approx \begin{cases} 1+(\frac{238}{40})^{\frac{1}{3}}0.081\,\ln(10\,x_U), & x\leqq x_U; \\ 1+(\frac{238}{40})^{\frac{1}{3}}0.081\,\ln(10\,x), & x_U<x<x_s; \\ 1.08-0.394\,x, & x_s\leqq x<x_m; \\ 11.7(x^2-x_m^2)-16.6(x-x_m)+0.80, & x_m\leqq x<1, \end{cases} \tag{30}$$

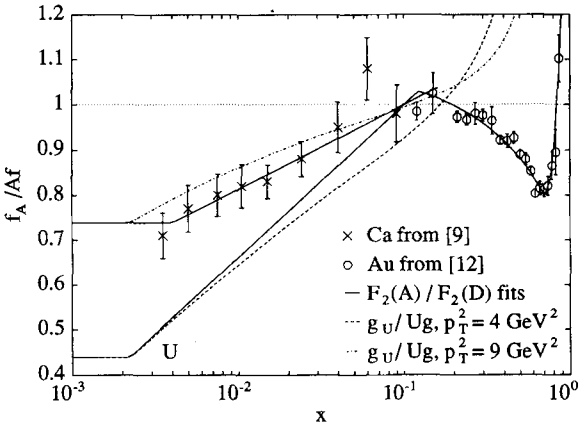

Fig. 5. The ratios $2F_2^A/AF_2^p$ and g_A/Ag as functions of the structure function x. The F_2-data for Ca at small x from [9] is shown with crosses and the respective data for Au at larger x from [12] with circles. The phenomenological fit to Ca F_2 data, as well as the extrapolation to U at small x, is illustrated with a solid line. The fit (30) for Au is directly used for U. The dashed line describes the two-gluon fusion corrected ratio g_A/Ag according to the initial state recombination model of [11] at the scale $Q^2=p_T^2=4$ GeV^2. In numerical computation of g_A (obtained by integration from (34)) we used the Woods-Saxon parametrization for nuclear densities and Duke-Owens soft gluon structure functions. In this model gluon corrections are strongly scale dependent and vanish rapidly with increasing p_T, as shown by the dotted-dashed line corresponding to $p_T^2=9$ GeV^2

where $x_s=0.122$ and $x_m=0.7$. This is illustrated in Fig. 5, where also the data mentioned above is shown, Ca with crosses and Au with circles. Since the data [9] does not show any significant scale dependence, we assume the form above to hold at all scales $p_T \geqq p_0$.

When writing the impact parameter dependent structure function for quarks and antiquarks we make the approximation that the F_2 ratio above gives the modifications to $\sum_f [q_f(x,p_T^2)+\bar{q}_f(x,p_T^2)]$ and that in the region $x \lesssim 0.1$ the correction term depends on the transversal location $\mathbf{s}$ (for a possible impact parameter dependent EMC region, see [26]). Proceeding similarly as for (9), we get the following expression

$$\Gamma_A^q(x,p_T^2,\mathbf{s}) \approx \sum_f [q_f(x,p_T^2)+\bar{q}_f(x,p_T^2)] \cdot T_A(\mathbf{s}) \cdot \left\{1+\frac{AT_A(\mathbf{s})}{N_A}[1-S_A^q(x)]\,\Theta(0.1-x) + [1-S_A^q(x)]\,\Theta(x-0.1)\right\}, \quad (31)$$

where $\Theta(x)=1$ when $x>0$ and 0 otherwise. As expected, the modifications in the region $x \gtrsim 0.1$ do not have a significant effect on the minijet production, especially when there is not any scale dependence in S_U^q. The effect on the jet numbers due only to (31) were checked to be a few per cent. As stated before, the shadowing corrections to the gluon structure functions at small x play a more important role.

There are several suggestions for the unknown nuclear modifications to the gluon structure function g_A [11, 18, 24, 25], of which we shall adopt the treatment in [11]. According to Close et al. initial state recombination at low scales Q^2 is mainly responsible for the shadowing and antishadowing corrections. The dominant contribution for gluons comes from the two-gluon fusion causing a correction to $Ag(x,Q^2)$ as

$$\delta g_A(x,Q^2) = \mathscr{C}(x,Q^2) \int dx_1\, dx_2\, g(x_1,Q^2)\, g(x_2,Q^2) \cdot \Gamma_{g_1g_2\to g}(x_1,x_2,x_1+x_2) \cdot [\delta(x-x_1-x_2)-\delta(x-x_1)-\delta(x-x_2)], \quad (32)$$

where the gluon-gluon fusion function is given by

$$\Gamma_{g_1g_2\to g}(x_1,x_2,x_1+x_2) = \frac{3}{4}\frac{x_1x_2}{(x_1+x_2)^2}\left(\frac{x_1}{x_2}+\frac{x_2}{x_1}+\frac{x_1x_2}{(x_1+x_2)^2}\right). \quad (33)$$

Nuclear geometry and scale dependence of the correction are contained in the factor $\mathscr{C}(x,Q^2)=(9A/8\pi R_A^2)(4\pi\alpha_s/Q^2)$. Since in the sharp surface sphere approximation $9A/8\pi R_a^2 = \int d^2\mathbf{s}\, T_A(\mathbf{s})\, T_A(\mathbf{s})$, the impact parameter dependent gluon structure function can be written as:

$$\Gamma_A^g x,p_T^2,\mathbf{s}) = T_A(\mathbf{s})\, g(x,p_T^2) + [T_A(\mathbf{s})]^2 \frac{4\pi\alpha_s(p_T)}{p_T^2} \cdot \int dx_1\, dx_2\, g(x_1,p_T^2)\, g(x_2,p_T^2)\, \Gamma_{g_1g_2\to g}(x_1,x_2,x_1+x_2) \cdot [\delta(x-x_1-x_2)-\delta(x-x_1)-\delta(x-x_2)], \quad (34)$$

where we can now use Woods-Saxon parametrization for nuclear density in $T_A(\mathbf{s})$. We expect this form to hold down to $x \sim x_U$, below which we take $\Delta\Gamma_U^g(x,p_T^2,\mathbf{s}) \approx \Delta\Gamma_U^g(x_U,p_T^2,\mathbf{s})$, i.e. again we assume the existence of a complete shadowing region. Also here by integration we get $g_A(x,p_T)=\int d^2\mathbf{s}\,\Gamma_A^g(x,p_T,\mathbf{s})$.

The ratio g_A/Ag is shown in Fig. 5. The dashed line corresponds to scale $p_T^2=4$ GeV^2 and the dotted-dashed

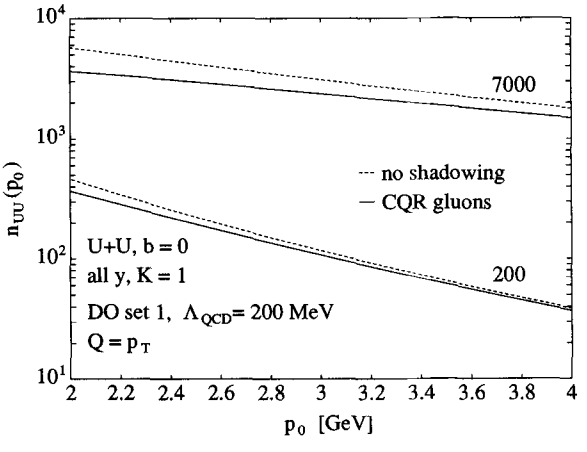

Fig. 6. The average number of jets with $p_T \geqq p_0$, any rapidity, from a central $U+U$ collision at $\sqrt{s}=7000$ AGeV and 200 AGeV, as computed from (10) with the structure functions (31) and (34) (solid lines). By "CQR gluons" we refer to the model in [11]. Here the suppression decreases clearly with increasing p_0, since the gluon correction vanishes as $\alpha_s(p_T)/p_T^2$. The estimates without shadowing are drawn with the dashed lines. Note that the horizontal p_0 scale is different from Fig. 1

one to 9 GeV^2. According to this model we get unrealistically increasing ratio for larger-x gluons. This is due to the fact that the initial state recombination model does not alone describe correctly the EMC-region. From our point of view, however, this does not matter, since the gluon densities at large x are already small as compared to the small x region.

In Fig. 6 we present the average number of jets with $p_T \geqq p_0$ as functions of p_0 at impact parameter fixed to $\mathbf{b}=\mathbf{0}$. As in Fig. 1 the jet numbers are computed for $\sqrt{s}=200$ and 7000 A GeV and all rapidities accepted (solid curves). The dashed curves are again the first order results from (1) for comparison. Nuclear shadowing reduces the central jet number by 20% for $p_0=2$ GeV at $\sqrt{s}=200$ A GeV and respectively by 36% at $\sqrt{s}=7000$ A GeV, the actual numbers being 368 and 3640. The suppression is in this case of the same order as for $K_U=0.3$ in Fig. 1.

Figure 7 shows the jet numbers averaged over all impact parameters, according to (11). These are as well plotted against p_0 for the two energies. The result obtained, 97 jets with $p_T \geqq 2$ GeV is 18% less than the jet number without any shadowing at $\sqrt{s}=200$ GeV. At $\sqrt{s}=7000$ GeV 982 jets with $p_T \geqq 2$ GeV are produced, and this is 33% less than the nonshadowed estimate.

Note that Figs. 6 and 7 show a clear difference to Figs. 1 and 3: shadowing is here strongly reduced with increasing p_0, whereas in Figs. 1 and 3 the shadowing correction to n_{UU} is nearly the same for all the p_0's shown. The answer to this different behaviour is simply the quite strong scale dependence ($\sim \alpha_s(p_T)/p_T^2$) of the gluon correction in (34). This decreases the correction term even if the typical x's are of the same order, $2p_0/\sqrt{s}$, for p_0's from 2 to 4 GeV. The results in the region below $p_0=2$ GeV are not shown, since the Duke-Owens parametrization with $Q=p_T$ should not be extrapolated far below $p_T=2$ GeV.

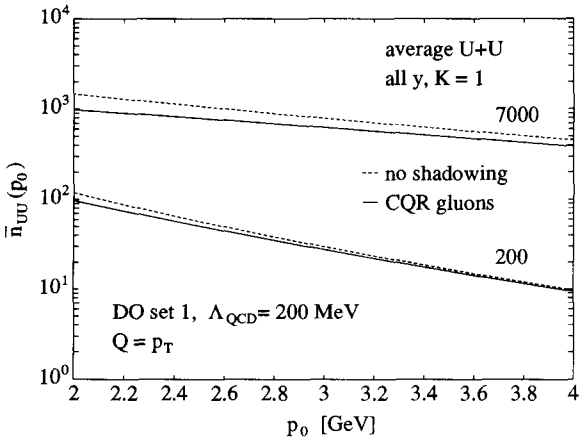

Fig. 7. The average number of jets with $p_T \geqq p_0$, any rapidity, from an average $U+U$ collision at $\sqrt{s}=7000$ A GeV and 200 A GeV, as computed from (11) with the impact parameter averaged structure functions, $US_U^2 \sum [q_f + \bar{q}_f]$ from (30) and g_A obtained by integration integrated from (34) (solid lines). The dashed lines show again the nonshadowed results

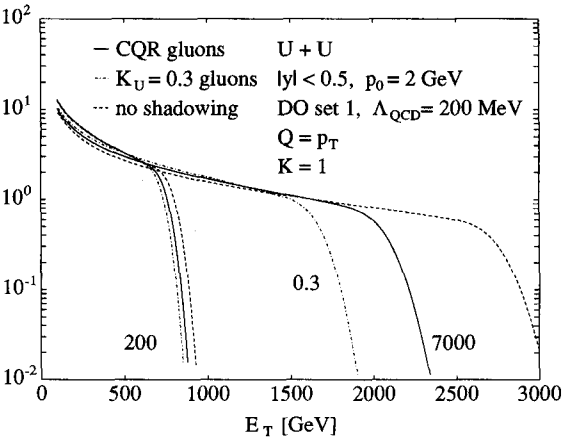

Fig. 8. The final transversal energy distribution for jets with $p_T \geqq 2$ GeV and $|y| \leqq 0.5$. Solid curves are the predictions where the hard moments were computed from (17) and (18) with the structure functions of Sect. 4. The soft contributions to these moments were added as in [2]. For comparison the nonshadowed estimates (dashed lines) and the $K_U=0.3$ result from Sect. 3 (dotted-dashed line) are also displayed

Since the shadowing corrections to the jet numbers with (31) and (34) are not as large as with (9), the central shadowing $C(p_0)$ cannot be a large effect, either. Indeed, this is the case, for $p_0=2$ GeV at $\sqrt{s}=7000$ A GeV it is only 6%, and at $\sqrt{s}=200$ A GeV it is less than a 3% effect. Practically, central shadowing has a significant role only if nuclear shadowing causes large reductions to the number of produced jets, as may be the case if the gluonic corrections turn out to be of the form (19).

Finally we compute the effects on the total E_T distribution from (16). This is plotted in Fig. 8 as a function of E_T under same acceptances as for Fig. 4, i.e. jets with $|y| \leqq 0.5$ and $p_T \geqq 2$ GeV were accepted. Again the distributions are computed for $\sqrt{s}=200$ and 7000 A GeV. The moments were calculated according to (17) and (18), no K-factors were used. The solid curve shows the result with the structure functions (31) and (34). We have also redisplayed the unshadowed curve (dashed) as well as the $K_U=0.3$ curve from Fig. 4 (dotted-dashed). In the present case we get on the average 23% less E_T at 7000 A GeV than in the nonshadowed case. The difference to the $K_U=0.3$ case is about 20% more in E_T, which results simply because the first moment (from (17)) is more weakly shadowed in the case of scale dependent corrections to the structure functions than in the scale independent case. At $\sqrt{s}=200$ A GeV the changes from the nonshadowed case are less than 10%, since the shadowing corrections are smaller and since the relative contribution of the soft part is larger.

6 Discussion and conclusions

In this paper, we have developed a formalism for impact parameter dependent structure functions with nuclear modifications at small x. We have thus given a framework for a quantitative study of the shadowing effects

combined to the effects of the collision geometry. By using two different models for the modifications to the parton structure functions in a nucleus we have applied our model to compute the average numbers of minijets and the transversal energy distribution in $U+U$ collisions. The formalism of this paper could be utilized in the event generators like HIJING [30], for a more detailed simulation of heavy ion collisions at very high energies.

In the EMC data for the structure function ratio $F_2(A)/F_2(D)$ there is a depletion at small x. It is natural to assume similar shadowing behaviour also for gluons, although one does not have any data for g_A/Ag, directly. Therefore we used two different models to describe g_A. Scale dependence of the shadowing corrections in g_A/Ag may play a crucial role: if the corrections *vanish* rapidly with the increasing scale $Q=p_T$, minijet production is clearly *less* suppressed than in the case where the corrections are scale independent.

With the impact parameter dependent structure functions we studied also the effects of collision geometry, i.e., how much more suppressed minijet production is in $\mathbf{b}\sim\mathbf{0}$ collisions than in the average ones. At LHC energies this central shadowing corresponded to about 10% reduction to E_T as compared to the case where the usual, shadowing corrected nuclear structure functions (but not impact parameter dependent) were used. This is the case if the modifications to g_A/Ag do not depend on the scale and the depth of the depletion in g_A/Ag is 50% at $x\leqq x_A$. At RHIC the central shadowing effect is only a few per cent. It is clear that central shadowing cannot be a large effect unless also shadowing effects are very large, since the impact parameter dependent structure functions are constrained to the 'usual' ones by integration over the impact parameter. We conclude, however, that the impact parameter dependence of the structure functions should be taken into account at LHC energies, where the shadowing effects in general are large.

Here we have studied the possible suppression on quark and gluon production caused by shadowing. In computing the cross sections we have applied only first order QCD perturbation theory. The order α_s^3 terms [22], which account for the so called K factor, can be large, increasing in pp collisions the number of minijets by a factor ~ 2.5 at RHIC energies [1, 2] and $\lesssim 2$ at Tevatron energies [1, 23] and perhaps by a smaller factor at LHC energies. The K factor depends at least on the experimental jet definition, on the scale Q used and on the structure function set used. This is why the K factor is hard to define in general. It is interesting to notice, however, that shadowing effects – depending on the behaviour of the gluon structure functions – may be of the same order as the contribution of the α_s^3-terms – but to an opposite direction.

The quantity which is still theoretically uncertain is the smallest p_T scale for the minijets. The dynamical meaning and the value of this scale is discussed in detail in [6]. It is, however, worth noticing that the effect of varying p_0 decreases when the energy is increased. This is seen e.g. in Fig. 6 where the number of jets with $p_T\geqq p_0$ is decreased by less than 35% when changing p_0 from 2 GeV to 3 GeV, while at RHIC energies the respective change would be 70%. Note that the K-factor and p_0 are bound together as far as the total cross sections for minijet production are conserned. With our choice $p_0=2$ GeV and $K=1$ the cross section $\sigma_{pp}(p_0)$ coincides with that in [16] at the Tevatron energy $\sqrt{s}=1800$ GeV (see [23]).

The general idea behind the heavy ion collisions at high energies is the study of strong interaction thermodynamics and a possible creation of quark-gluon plasma. The energy density necessary for the deconfinement phase transition is $\varepsilon_c\sim 1-3$ GeV/fm^3. According to Figs. 4 and 8 we find the Bjorken estimate of the energy density [27] at the formation time scale $\tau_0\sim 1$ fm to be $\varepsilon_{Bj}=6-12$ GeV/fm^3 at LHC and ~ 4 GeV/fm^3 at RHIC, including the shadowing effects discussed in this paper. These estimates coincide with values given in [28]. Thus the obtainable energy densities stay above ε_c, in spite of the suppression caused by shadowing.

To conclude, after this study we have a better handle on the magnitude of the shadowing effects on minijet production. In this study we have presented a framework for including the shadowing effects; even more reliable results can be obtained after one gets more information from the forthcoming heavy ion experiments at RHIC and at CERN.

Acknowledgements. The author thanks K. Kajantie for suggesting the study of this subject and J. Lindfors, P. Castorina, S. Gavin, S. Gupta, M. Gyulassy, A. Mueller and X.-N. Wang for helpful discussions. The financial support by the Academy of Finland, E.J. Sariola foundation, Alfred Kordelin foundation and Jenny and Antti Wihuri foundation is acknowledged as well as the hospitality of the Institute for Nuclear Theory, University of Washington.

References

1. UA1 Collab., C. Albajar et al.: Nucl. Phys. B309 (1988) 405; F. Abe et al.: Phys. Rev. Letters 62 (1989) 613
2. K.J. Eskola, K. Kajantie, J. Lindfors: Nucl. Phys. B323 (1989) 37
3. K. Kajantie, P.V. Landshoff, J. Lindfors: Phys. Rev. Lett. 59 (1987) 2527
4. K.J. Eskola, K. Kajantie, J. Lindfors: Phys. Lett. B214 (1989) 613
5. K.J. Eskola, J. Lindfors: Z. Phys. C – Particles and Fields 46 (1990) 141
6. L.V. Gribov, E.M. Levin, M.G. Ryskin: Phys. Rep. 100 (1983) 1; E.M. Levin, M.G. Ryskin: Nucl. Phys. B304 (1988) 805; J.-P. Blaizot, A.H. Mueller: Nucl. Phys. B289 (1987) 847; T. Sjöstrand, M. van Zijl: Phys. Rev. D 36 (1987) 2019
7. K.J. Eskola: Proc. Quark Matter '90, J.P. Blaizot, C. Gerschel, B. Pire, A. Romana (eds.). Nucl. Phys. A525 (991) 393c
8. EM Collab., J. Ashman et al.: Phys. Lett. B202 (1988) 613; EM Collab., M. Arneodo et al.: Phys. Lett. B211 (1988) 493; D.M. Alde et al.: Phys. Rev. Lett. 64 (1990) 2479
9. EM Collab., M. Arneodo et al.: Nucl. Phys. B333 (1990) 1
10. P. Castorina, A. Donnachie: Z. Phys. C – Particles and Fields 45 (1989) 141
11. F.E. Close, J. Qiu, R.G. Roberts: Phys. Rev. D40 (1989) 2820
12. R.G. Arnold et al.: Phys. Rev. Lett. 52 (1984) 727
13. D.W. Duke, J.F. Owens: Phys. Rev. D30 (1984) 49
14. B.L. Combridge, C.J. Maxwell: Nucl. Phys. B239 (1984) 429; F. Halzen, P. Hoyer: Phys. Lett. B130 (1983) 326

15. Jianwei Qiu: Nucl. Phys. B291 (1987) 746
16. I. Sarcevic, S.D. Ellis, P. Carruthers: Phys. Rev. D40 (1989) 1446
17. E.L. Berger, J. Qiu: Phys. Lett. B206 (1988) 41; F.E. Close, R.G. Roberts: Phys. Lett. B213 (1988) 91
18. L.L. Frankfurt, M.I. Strikman: Phys. Rep. 160 (1988) 237; L.L. Frankfurt, M.I. Strikman: Nucl. Phys. B316 (1989) 340; L.L. Frankfurt, M.I. Strikman, S. Liuti: Rev. Lett. 65 (1990) 1725
19. J. Kwiecinski: Z. Phys. C – Particles and Fields 45 (1990) 461
20. S. Brodsky, H.J. Lu: Phys. Rev. Letters 64 (1990) 1342
21. A. Bohr, B.R. Mottelson: Nuclear Structure I, pp. 160, 223, New York: W.A. Benjamin, Inc. 1969
22. R.K. Ellis, J.C. Sexton: Nucl. Phys. B269 (1986) 445; S. Ellis, Z. Kunszt, D. Soper: Phys. Rev. Lett. 64 (1990) 2122
23. K.J. Eskola: Proc. of European Committee for Future Accelerators/Large Hadron Collider Workshop, 1990, G. Jarlskog, D. Rein (eds.) CERN 90-10, ECFA 90-133, vol. II, p.1195
24. J. Collins, J. Kwiecinski: Nucl. Phys. B335 (1990) 89
25. A.H. Mueller, Jianwei Qiu: Nucl. Phys. B (1986) 427
26. P. Castorina, A. Donnachie: Z. Phys. C – Particles and Fields 49 (1991) 481
27. J.D. Bjorken: Phys. Rev. D27 (1983) 140
28. U. Heinz: Proc. of European Committee for Future Accelerators/Large Hadron Collider Workshop, 1990, G. Jarlskog, D. Rein (eds.) CERN 90-10, ECFA 90-133, vol. II, p. 1079
29. K. Werner: Proc. of European Committee for Future Accelerators/Large Hadron Collider Workshop, 1990, G. Jarlskog, D. Rein (eds.) CERN 90-10, ECFA 90-133, vol. II, p. 1098; L. Ramello: Prov. of European Committee for Future Accelerators/Large Hadron Collider Workshop, 1990, G. Jarlskog, D. Rein (eds.) CERN 90-10, ECFA 90-133, vol. II, p. 1115
30. X.-N. Wang, M. Gyulassy: University of California preprint LBL-29390